Atomic String Holography

J. C. H. Spence* and C. Koch
Department of Physics and Astronomy, Arizona State University, Tempe, Arizona 85287
(Received 31 January 2001)

A new diffraction-channeling effect has been discovered, in which Kikuchi or channeling line patterns formed by high energy electrons, neutrons, and positrons are shown to break up into a series of annular disks if the crystal thickness traversed by the beam is small. The disks may be interpreted as Gabor in-line holograms of strings of atoms projected along the beam path. For electrons or positrons the patterns may be detected with little background by detecting characteristic x-ray emission from a thin film as a function of the diffraction conditions of a collimated, ionizing, high energy beam. Uses of the effect for structure determination and atomic-resolution lensless imaging are suggested.

DOI: 10.1103/PhysRevLett.86.5510 PACS numbers: 61.14.Nm, 87.64.Bx

A considerable scientific payoff could be expected from the development of a general method of obtaining near-field images from the intensity of scattered radiation. By avoiding the aberrations and resolution limits introduced by lenses, and by allowing imaging with radiations for which no lenses exist, such a method could be expected to contribute greatly to our understanding of phenomena as diverse as protein folding, nano and mesoporous structure analysis, catalysis, and nucleation, and growth processes in surface science. The use of new radiations, such as coherent atom beams and neutrons, for imaging [1] may then open up new possibilities for minimizing radiation damage to biomolecules [2]. The associated inversion problem from scattering to image was therefore attacked by many of the leading scientists of the last century, from Rutherford and Gabor to those who solved the phase problem of x-ray crystallography by direct and other methods. Recently a variety of schemes which allow a holographic interpretation of fluorescent x rays (or photoelectrons) have appeared [3]. These depend on the use of atoms in similar local environments as internal "point" emitters (or detectors) of radiation, each producing identical in-line holograms of the local environment on a distant detector [4,5]. Translational symmetry between source or detector atoms is not required. These schemes may be classified according to the type of radiation and beam energy used, which determine the elastic and inelastic scattering lengths and hence the surface or bulk sensitivity. Interpretation is simplified, and intensity maximized, if either the incident or emitted radiation is nondiffracting—this may be achieved using a large illumination/detector angle, a wide range of energies, or a layer of material thinner than the elastic scattering length. The possibilities may be written, e.g., $(\gamma, \underline{e})$, with incident particle first and diffracting particle underlined. Application of reciprocity to the diffracting channel reverses the order of symbols and underline. Of the resulting eighteen possibilities (including neutrons), several remain untried, while the background of nondiffracting processes and kinematic constraints otherwise limit possibilities. In related techniques such as holographic LEED [6] and the heavy atom method of x-ray crystallography, there is negligible energy change on scattering. Twin images (see DeVelis *et al.* [7] for the first solution to this problem) and multiple scattering are minimized by integration over beam energy [3,5]; however, for electrons, variations in the phase of the reference wave with angle and forward-focusing may introduce artifacts (but see [8]). X-ray methods do not suffer from these difficulties, but scatter weakly; however, the $(\underline{\gamma}, \gamma)$ (IXFH) method, using a pink beam, greatly reduces recording time. The relevant history of ideas includes the Borrman effect [9], and the structural information it contains [10] in addition to the theory of Kossel and Kikuchi lines [11]. Gabor's in-line holography is also relevant; however, it was intended for systems without symmetry. The first observation of the dependence of fluorescence on diffraction conditions may be that of Knowles [12], using diffracting neutrons $(\underline{n}, \gamma)$. Holographic reconstruction from internal sources was demonstrated with gas diffraction by Bartell [13]. Atomic resolution has recently been achieved using external-source, off-axis electron holography [14], in fulfillment of Gabor's original aim, to correct the aberrations of an electron microscope holographically.

The purpose of this Letter is to describe a new $(\underline{e}, \gamma)$ holographic diffraction method which uses high energy (300 kV) electrons traversing a thin crystalline slab to produce lensless, three-dimensional imaging of the internal atomic structure of the film. Characteristic x rays are detected as a function of the angle of a coherent electron beam, which excites the x rays and is weakly refracted by atomic strings in the crystal. The x rays are not diffracted due to the small film thickness.

Figure 1(a) shows our geometry. A thin crystal, about 10 nm thick, is used, as for atomic-resolution TEM. A high energy (e.g., 300 keV) collimated electron beam traverses the crystal slab, exciting x-ray fluorescence from the Cl atoms of the bcc CsCl structure shown. The thickness is less than an extinction distance for Bragg scattering, so that electron standing waves do not build up inside the crystal to modulate fluorescence, as in the "Alchemi" technique

 0031-9007/01/86(24)/5510(4)$15.00

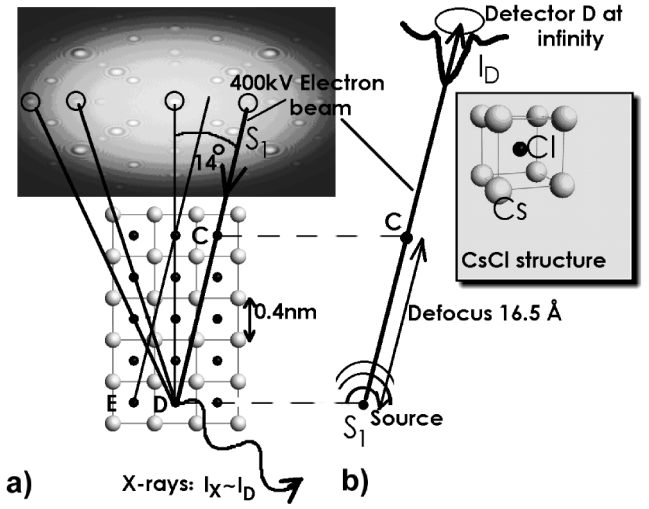

FIG. 1. Atomic-string holography at high electron energies. (a) Incident beam running along atomic columns excites fluorescence, whose total yield is mapped above as a function of incident beam direction. Atomic columns corresponding to spots in the pattern can easily be identified. (b) Time-reversed point source of high energy electrons produces similar pattern. Inset shows CsCl bcc structure.

used to locate foreign atoms in thin crystals [15]. The x-ray intensity emitted by atom D is proportional to the intensity I_D of the diffracted electron intensity at D due to the external source S_1 [16], if localization effects are negligible (x-ray energies above about 500 eV [17]). Applying reciprocity to this arrangement, we see in Fig. 1(b) that I_D equals the intensity at infinity from a point source of 300 kV electrons within the sample at D. This intensity variation with angle is an in-line hologram of atom C as formed by a point source at D with "defocus" (source to sample distance) DC, shown in Fig. 1(a). There is one hologram for every atomic column or string along the optical path between source and detector. Every string parallel to the one shown [e.g., at E in Fig. 1(a)] generates an identical hologram, whose intensity distributions must be added together, since the x-ray "detection" process is incoherent. For sufficiently thin films the individual holograms from nonparallel atomic columns are spatially separated on the detector, since the angles between strings are relatively large. Where a mixture of species occurs along such a path, a sum must be taken over all the reciprocal "sources" in Fig. 1(b) defined by the x-ray energy, and over the atoms imaged along the path. Unlike low energy electron holography, the electron scattering process is highly forward-peaked, with a strong concentration of energy along atomic strings. For thicknesses t small enough to avoid overlap of holograms, the atoms on a string act as phase objects, and the contrast at the detector arises from the "out-of-focus" propagation over the distance $\Delta z = DC$. This distance creates contrast in the image of the phase-object atom at C, which appears as a variation in x-ray emission with angle. For thicker samples, progressing from two-dimensional to three-dimensional diffraction and associated momentum conservation laws, the holograms overlap and eventually form a Kikuchi pattern. In thin samples the method generates the holograms of atomic strings which would be produced by a 300 kV internal point source of electrons, on a distant detector. This energy is sufficiently high to ensure that there are no multiple-scattering artifacts. The wide angular range of illumination directions possible under computer control in TEM provides projections from many angles, overcoming the limitation of off-axis electron holography to two-dimensional reconstruction [14]. Because HEED is strongly forward-scattered, reconstruction from a single hologram cannot distinguish different planes along the beam path, as in the Barton algorithm, due to the rapid falloff in angle for HEED scattering factors.

To test these ideas we have performed detailed multiple-scattering calculations for 1 MeV electrons traversing a thin crystal of CsCl. The Cl x-ray fluorescence which results is taken to be proportional to the intensity of the electron beam wave field on the Cl site (all such sites are equivalent). For computational convenience, we use the reciprocal arrangement, and launch a spherical wave within the crystal from one Cl atom. A relativistically corrected one-electron Schrödinger equation is solved for the propagation of this wave through the crystal, using the multislice superlattice method [18]. The scattering potential is synthesized from relativistic Hartree-Fock calculations for atoms, and all orders of multiple scattering are included, with Debye-Waller factors for room temperature. Figure 2 shows the resulting elastic scattering for 1 MeV electrons on a screen at infinity, plotted as a function of angle, and a model of the CsCl crystal as seen by the source atom (atom C) in Fig. 1), which is at the center of the image, above the plane of the page. The intensity in the hologram is proportional to the total Cl characteristic x-ray emission, as a function of the incident beam direction. We note that the number of atomic holograms along each radial line is

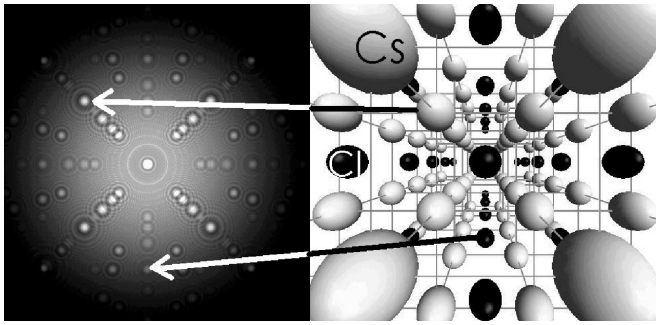

FIG. 2. Left: Multiple scattering produced by point sources of 1 MeV electrons on Cl atoms in a thin film of CsCl (7 monolayers thick). Each blob in the figure lies over an atomic position in the perspective diagram of the crystal structure shown at right. The source atom lies above the plane of the paper and is not shown.

just equal to the number of atoms seen in perspective. The figure confirms that separate holograms are obtained for every atomic string, in the form of a central maximum surrounded by a Fresnel fringe. These holograms are seen to fall in one-to-one angular correspondence with rays drawn along the prominent atomic columns or strings in the structure from the source atom, as shown in Fig. 1.

A simple interpretation of these holograms is possible if the approximation is made that the potential is zero between the emitter atom and the imaged atom. Then, for atoms spaced by Δz along the string, each atomic string hologram can be shown to be identical (apart from magnification) to that which would be produced on a screen placed a distance Δz beyond an atom illuminated by a plane wave [18]. (This follows from the equivalence of the point-projection and plane-wave geometries.) In this sense the hologram is an image, out-of-focus by Δz. Hence these holograms have the form

$$I(r) = |q(r) * * t(r)|^2,$$

where $q(r) = \exp(-i\sigma\phi_p(r))$, $\phi_p(r) = \int \phi(r)\, dz$, and $t(r) = \exp(-i\pi r_2/(\Delta z \cdot \lambda))$ is the free-space propagator or Green's function. The $**$ denotes convolution, $\phi(r)$ is the electrostatic or Coulomb potential for the atom, and $\sigma = \pi/\lambda V$ is the interaction constant for an electron beam of energy eV. The integral is taken antiparallel to the beam path from an origin on the x-ray emitting atom. Since these are not Fraunhoffer holograms ($\Delta z < d^2/\lambda$, d the diameter of the atom [7]), reconstruction of the holograms would encounter a twin image problem, which is soluble in principle by varying the energy of the beam over a range which changes the Fresnel number $N = r^2/(\Delta z \times \lambda \times 2)$ by 0.5. In practice, the direct resemblance of the patterns to a projection of the real-space crystal structure from an atom identified by its characteristic radiation will be sufficient to solve it. From thicker regions, conventional electron diffraction methods can be used to determine the periodicity along the atomic strings, using high-order Laue zone lines, the space group, and lattice spacings [18].

Since the spatial resolution of these images greatly exceeds that of current TEM imaging techniques, their sensitivity to atomic number and ionic state is of interest. Consistent with the first-order expansion of $q(r)$, we find that neighbors in the atomic table can be distinguished in the absence of background, and that, for example, the intensity at the center of Cs (55) is 3 times that at the center of the Cl (17) hologram. Br (35) is about twice Cl. This axial intensity is the most sensitive point to the charge state of the ions, since it involves forward electron scattering, which tends to infinity for an unscreened isolated ion [18].

Figure 3 shows how the contrast of the string holograms is inverted for positrons as incident particles and how the patterns vary with increasing thickness, first to a projection of the structure at moderate thickness, and finally to the familiar Kikuchi patterns at large thickness, due to localized

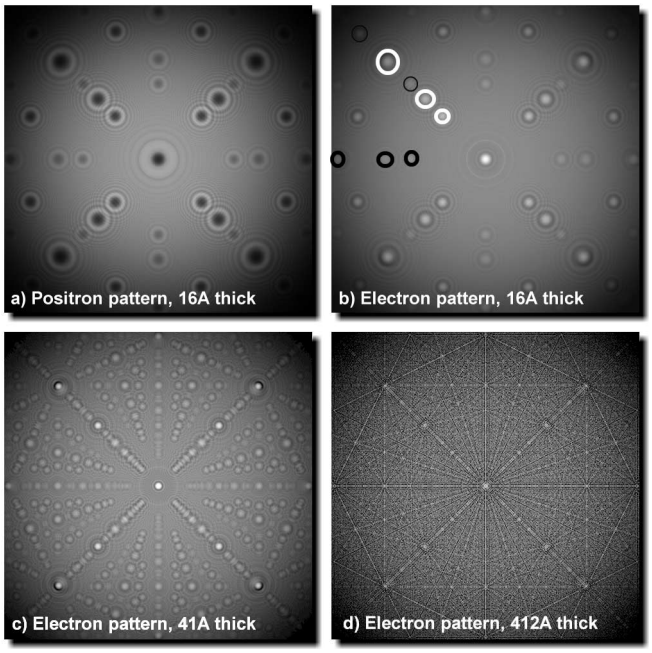

FIG. 3. (a) 1 MeV positron hologram. (b)–(d) 1 MeV electron holograms for samples of different thicknesses. The displayed intensity is the sum of holograms due to sources at every depth up to the sample thickness. In (b) the different holograms of Cs and Cl atoms are indicated by white and black circles, respectively (compare with Fig. 2 for position of all the holograms).

phonon (quasielastic) scattering. The transition to a spotty pattern at small thickness was evidently overlooked by the discoverers of Kikuchi and Kossel patterns, which result from three-dimensional diffraction satisfying Bragg's law on the surfaces of cones [11]. In Fig. 3, however, both radial and nonradial K lines remain. Radial lines are seen in channeling star patterns at much higher energies, due to a lack of angular resolution, but are not seen in the high angular resolution patterns obtained at sub MeV energies. Evidently the forward focusing effect, which produces the radial lines, becomes ineffective for longer strings, as the focusing distance gets out of step with the interatomic spacing [19]. These atomic focusing effects have also been observed at high energy [20]. Thus an atom in the path of a kilovolt electron beam acts as a lens, with a focal length of a few nm, depending on beam energy. Hence special accelerating voltages may be chosen to enhance the intensity or vary the magnification of string holograms.

The spatial resolution of the method depends on several factors, including the vibrational amplitude of the source atom Δr, the inelastic localization $L \sim \lambda/\Theta_E$ [21,22], and the divergence of the electron beam (which limits intensity). Here Θ_E is the mean inelastic scattering angle, and L is a quantum equivalent of an impact parameter. Since no static displacement is possible between source and imaged atom (as in field-ion microscopy), mechanical vibration does not limit resolution, as in other atomic-resolution microscopies. For x-ray energies greater than 1 kV, $L < 0.1$ Å. By reciprocity, the effect of a finite

electron beam divergence $\Delta\theta$ is to smear out detail in the hologram over this angular range. Typical divergences of milliradians are very much smaller than the width of the inner Fresnel fringes. The resolution in the final reconstruction is about equal to the width of the finest Fresnel fringe observed. The angular smearing due to thermal vibration is $\Delta r/2\Delta z \approx 2.5$ mRad at room temperature, which sets an upper limit on beam divergence and hence exposure time. Cooling thus increases resolution only if divergence is reduced commensurately, and exposure time increased.

Experimental observation of atomic string holograms requires the same TEM apparatus used for "Alchemi," but thinner crystals. Using a 200 nm diameter electron beam (LaB6 source), with $\Delta\theta = 1.8$ mRad, in samples 200 nm thick, Rossouw *et al.* [23] collected statistically significant standing-wave fluorescence (Alchemi) data on a 79×58 pixel array in 2 h (0.3 sterad x-ray detector, 30 mm^2). For the 10 nm thick films required for string holography, this time becomes 5 h using four of the new 60 mm^2 detectors, or 13 min for one hologram. Current TEM/STEM instruments are not optimized for these experiments and allow many improvements.

In summary, we have discovered a new channeling effect for very thin crystals, overlooked within previous theories of Kikuchi lines. The patterns, interpreted as holograms, solve the multiple-scattering problems of earlier methods, while ensuring adequate signal, and providing true three-dimensional information. For bulk samples, the possibility arises of applying this method to a beam whose energy is chosen slightly above the x-ray ionization threshold, thereby limiting the information depth to the inelastic mean free path. This requires the use of a localized excitation with short ($<$10 nm) inelastic mean free path. The coherent probe formed over very large angles by an aberration-corrected STEM may also be expected to form these patterns. A two-dimensional array of orientationally ordered organic molecules [24] containing a single fluorescing species or a semiconductor overlayer would also produce string holograms. Similar string holograms can be expected from incoherent neutron Kikuchi patterns [1,25] in thin samples, since the scattering is isotropic. Radiation damage effects on biological samples can then be small [2].

Thanks to J. M. Cowley and M. van Hove for discussions. Supported by NSF Grant No. DMR9814055.

*Email address: spence@asu.edu

[1] B. Allman, P. McMahon, K. Nugent, D. Paganin, D. Jacobson, M. Arif, and S. Werner, Nature (London) **408**, 158 (2000).
[2] R. Henderson, Q. Rev. Biophys. **28**, 171 (1995).
[3] G. Feigel and M. Tegze, Rep. Prog. Phys. **62**, 355 (1999).
[4] A. Szoke, in *Short Wavelength Coherent Radiations,* AIP Conf. Proc. No. 147 (AIP, New York, 1986).
[5] J. Barton, Phys. Rev. Lett. **67**, 3106 (1991).
[6] D. Saldin, Surf. Rev. Lett. **4**, 991 (1997).
[7] J. B. DeVelis, G. Parrent, and B. Thompson, J. Opt. Soc. Am. **56**, 423 (1966).
[8] J. Wider, F. Baumberger, M. Sambi, R. Gotter, A. Verdini, F. Bruno, D. Cvetko, A. Morgante, T. Greber, and J. Osterwalder, Phys. Rev. Lett. **86**, 2337 (2001).
[9] M. von Laue, Acta Crystallogr. **2**, 106 (1949).
[10] J. Cowley, Acta Crystallogr. **17**, 33 (1964).
[11] S. Kikuchi, Jpn. J. Phys. **5**, 83 (1928).
[12] J. Knowles, Acta Crystallogr. **9**, 61 (1956).
[13] L. Bartell and C. L. Ritz, Science **185**, 1163 (1974).
[14] A. Orchowski, W. Rau, and H. Lichte, Phys. Rev. Lett. **74**, 399 (1995).
[15] J. Spence and J. Tafto, J. Microsc. **130**, 147 (1982).
[16] D. Cherns, A. Howie, and M. Jacobs, Z. Naturforsch. A **28**, 565 (1973).
[17] W. Qian, B. Totdal, R. Hoier, and J. Spence, Ultramicroscopy **41**, 147 (1992).
[18] J. Spence and J. Zuo, *Electron Microdiffraction* (Plenum, New York, 1994).
[19] M. van Hove (personal communication).
[20] J. Cowley, J. Spence, and V. Smirnov, Ultramicroscopy **68**, 135 (1997).
[21] J. Spence, in *High Resolution Electron Microscopy,* edited by C. Buseck and L. Eyring (Oxford University Press, New York, 1988).
[22] A. Howie, J. Microsc. **117**, 11 (1979).
[23] C. Rossouw, C. Forwood, M. Gibson, and P. Miller, Philos. Mag. A **74**, 57 (1996).
[24] J. Larson, K. Hald, N. Bjerre, and H. Stapelfeldt, Phys. Rev. Lett. **85**, 2470 (2000).
[25] S. Dudarev, Kristallografiya **35**, 596 (1990).